Vehicle Engine Torque Estimation via Unknown Input Observer and Adaptive Parameter Estimation

Jing Na, *Member, IEEE*, Anthony Siming Chen, Guido Herrmann, *Senior Member, IEEE*, Richard Burke, and Chris Brace

***Abstract*—This paper presents two torque estimation methods for vehicle engines: unknown input observer (UIO) and adaptive parameter estimation. We first propose a novel yet simple unknown input observer based on the crankshaft rotation dynamics only. For this purpose, an invariant manifold is derived by defining auxiliary variables in terms of first-order low-pass filters, where only one constant (filter coefficient) needs to be tuned. These filtered variables are used to calculate the estimated torque. Robustness of this UIO against sensor noise is studied and compared to two other estimators. On the other hand, since the engine torque dynamics can be formulated as a parameterized form with unknown time-varying parameters, we further present several adaptive laws for time-varying parameter estimation. The parameter estimation errors are derived to drive these adaptive laws and time-varying adaptive gains are introduced. The two proposed estimators only use the measured air mass flow rate and engine speed, and thus allow for improved computational efficiency. Both estimators are verified via a dynamic engine simulator built in a commercial software GT-Power, and also practically tested via experimental data collected in a dynamometer test-rig. Both simulations and practical tests show very encouraging results with small estimation errors even in the presence of sensor noise.**

***Index Terms*—Engine torque estimation, mean value engine model, time-varying parameter estimation, unknown input observer.**

I. Introduction

In THE past decades, many efforts have been made on the integration and development of modern vehicular systems driven by internal combustion (IC) engines and electric motors. The complexity of such vehicular systems has created challenges in the engine management system (EMS), especially for sensor integration. In the new generation of EMS and other vehicle powertrain control, the effective engine torque has been found to be one of the crucial variables, which has been used in various automotive applications, e.g., online estimation of in-car parameters such as mass [1], brake torque control [2], speed control [3], on-board diagnostics [4], and even hybrid electric vehicle applications [5], [6].

In a laboratory environment, the effective engine torque can be calculated by using the measured cylinder pressure with an in-cylinder pressure sensor [7]. However, this idea is usually impractical in commercial cars due to the high sensor cost and the complicated configuration. Hence, it is necessary to exploit indirect methods to measure engine torque, i.e., estimate the unknown engine torque based on the other easily measurable variables.

Among various torque estimation strategies, the most commonly used ones are lookup tables with engine speed, intake manifold pressure, spark advance, and injected fuel, etc., which have been built via time-consuming offline calibrations [7]. To reduce the cost and period of offline calibrations, the relationship between the engine torque and other engine variables, e.g., throttle angle and speed, are further considered, and various observer designs have been used. On this topic, early-stage work was carried out using a sliding mode observer based on the crankshaft model [8]–[10], where the engine speed fluctuations are used to determine the effective torque based on an electrical circuit model [8]. Recently, the principle of high order sliding mode observer designed based on a super-twisting algorithm has also been studied in [11] and [12] for estimating the engine parameters that are related to engine torque, i.e., friction torque and load torque. Chauvin *et al.* [13], [14] proposed two different torque estimation approaches for diesel engines using an adaptive Fourier basis decomposition observer [13] and a time-varying Kalman filter [14]. The estimators only used the engine speed sensor, however, the engine dynamics were assumed to be known, which may not be true in practical applications. To address unknown parameters, an adaptive Kalman filter was proposed in [3] to estimate the load torque for SI engines. In the work of Falcone *et al.* [15], [16], the torque estimation was reformulated as a tracking control problem and solved using a linear quadratic (LQ) optimal control. To further diminish sensitivity to the crankshaft model uncertainties, Helm *et al.* [4] proposed a PI-like observer. In Hong *et al.* [17], a cascade estimator was proposed to estimate the real-time torque by using available information from the stock engine sensors, e.g., intake

Manuscript received January 24, 2017; revised July 2, 2017; accepted July 31, 2017. Date of publication August 14, 2017; date of current version January 15, 2018. This work was supported by the Marie Curie Intra-European Fellowships Project AECE under Grant FP7-PEOPLE-2013-IEF-625531, the National Natural Science Foundation of China under Grant 61573174, and a joint PhD Scholarship between Chinese Scholar Council and University of Bristol under Grant 201708060062. The review of this paper was coordinated by Dr. D. Cao. *(Corresponding author: Jing Na.)*

J. Na is with the Faculty of Mechanical and Electrical Engineering, Kunming University of Science and Technology, Kunming 650500, China (e-mail: najing25@163.com).

A. S. Chen and G. Herrmann are with the Department of Mechanical Engineering, University of Bristol, Bristol BS8 1TR, U.K. (e-mail: sc15280.2014@my.bristol.ac.uk; G.Herrmann@bristol.ac.uk).

R. Burke and C. Brace are with the Powertrain Vehicle Research Centre, Department of Mechanical Engineering, University of Bath, Bath BA2 7AY, U.K. (e-mail: R.D.Burke@bath.ac.uk; C.J.Brace@bath.ac.uk).

Color versions of one or more of the figures in this paper are available online at http://ieeexplore.ieee.org.

Digital Object Identifier 10.1109/TVT.2017.2737440

pressure, engine speed. In this observer, the difference between the measured engine speed and the observed speed is derived to online modify the torque, and the intake pressure is used to calculate a nominal torque. These observers either require precise engine models or impose coupled observers with many tuning parameters, and thus the estimation results may not be accurate and fast during transient conditions.

On the other hand, another approach to estimate the engine effective torque is to take this torque as a virtual input of the torque production dynamics, and then to use the principle of unknown input observer (UIO) [18], [19]. In particular, Stotsky and Kolmanovsky [18] investigated several UIOs, and their application to engine torque estimation was also studied with cascade schemes. The adaptive version of a high gain observer given in [18] was presented in [19], where the unknown parameters of engines were estimated and then used to calculate the engine torque. In this case, the engine torque estimation problem can be studied via parameter estimation schemes because the engine torque generation dynamics can be appropriately parameterized in a quasilinear form, which is also used in [17]. However, the parameters involved in this quasilinear formulation are time-varying rather than constant, i.e., the thermal efficiency and volume efficiency are not constant. Consequently, the classical parameter estimation methodologies (e.g., gradient descent, least squares [20], [21]) are not able to deal with the engine torque estimation due to the fast time-varying parameters in the torque production dynamics. In fact, the time-varying parameter estimation has not been fully solved in the field [22]. A recent solution was proposed in [23], where a set-membership algorithm was incorporated into the input observer. However, the estimation performance depends on the knowledge of precise bounds for the unknown parameters. To tackle above mentioned issues, our preliminary work [24] presented an improved UIO and a parameter estimator with guaranteed convergence.

In this paper, we address the engine torque estimation by proposing two fast and robust estimation algorithms: unknown input observer and adaptive time-varying parameter estimation. The first algorithm is designed based on the engine rotation dynamics only. Low-pass filter operations are first applied to the measured engine speed and load torque; these filtered variables then indicate an implicit relationship between the filtered variables and the unknown engine torque based on the idea of an invariant manifold [27]. This provides a simple and robust UIO, which guarantees exponential error convergence. Theoretical analysis of the ultimate error bounds and the robustness of three different UIOs are also provided. The second method is designed by considering the fact that the unknown torque is a function of some engine variables as [17], which can be easily measured (e.g., air mass flow rate and engine speed), and thus it can be reformulated in a quasilinear form [24] subject to time-varying parameters. Then, we can calculate the engine torque by using the estimates of these time-varying parameters. Thus, this proposed estimator is developed by modifying a recent idea for adaptive parameter estimation [28], [29]. In particular, we use the parameter estimation error to drive the adaptive laws and suggest time-varying learning gains, such that the convergence can be trivially proved under a generic persistent excitation (PE) condition [30], and faster convergence response can be achieved. It is noted that the proposed algorithms are very generic; they can be used for different engines including naturally aspirated port fuel injected petrol engine, turbocharged direct fuel injected petrol engine and turbocharged direct fuel injected diesel engine. These three engine types represent the majority of the passenger vehicles while the latter two represent the trend for future engines.

For the theoretical development, the widely-used mean value engine model (MVEM) proposed by Hendricks *et al.* [25], [26] is considered. However, the two proposed estimators are verified based on different simulation and experimental data sets. Thus, we first test our methods in an 1D environment, where a port fuel injected Spark Ignition (SI) engine model built in a professional engine simulation software, GT-Power [31], is used. This model is more realistic than the MVEM because the real torque oscillations as a result of the firing of each cylinder are simulated. Artificial measurement noise is also adopted to verify the sensitivity of the proposed algorithm against noise. Finally, we demonstrate the effectiveness via experimental data sets from practical tests based on a dynamometer test-rig of direct injection diesel engine. These tests include the real torque oscillations and a number of measurement inaccuracies. Both simulation and practical tests show very good results with small estimation errors.

This paper is organised as follows. Section II describes the engine dynamics. Section III proposes a UIO design and comparisons to other two methods. Section IV gives the robustness analysis. Section V presents several adaptive laws for time-varying parameter estimation. Simulations based on a well-calibrated GT-Power engine model are provided in Section VI and practical results are given in Section VII. Section VIII provides a comparative discussion and Section IX some conclusions.

II. Vehicle Engine Modeling and Problem Statement

This section will introduce the dynamics of IC engine systems. Note that the general work principle of both Spark Ignition (SI) and Compression Ignition (CI) engines is that the combustion of air-fuel mixtures in the chambers produces the driving torque for crankshaft rotation. The air mass flow and the injected fuel into the intake manifold and engine chamber can be controlled accordingly (e.g., stoichiometric for SI engines or lean mixture for CI engines). Nevertheless, the crankshaft dynamics will be the basis to the estimation schemes in this paper. Hence, to demonstrate this we present here the major blocks of a port-injected engine as in Fig. 1.

It can be found from Fig. 1 that the engine system can be divided into several sub-systems: air path system, fuel path system, torque production system and crankshaft system [25], [26]. In general, modelling of engine system is not a trivial task because of its nonlinear and time-varying behaviours. Among various modelling methods, a physical based model called mean value engine model (MVEM) has been widely used [25], [26], which can calculate the average variables accounting for the thermodynamics, fluid mechanics and rigid body dynamic over several engine operation regimes. This model is relatively simple

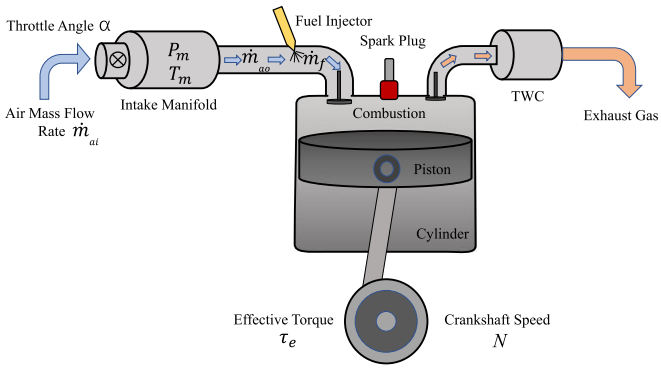

Fig. 1. Simplified sketch of SI engine systems.

TABLE I
ENGINE VARIABLES USED IN THE MODEL

Symbol	Variable	Symbol	Variable
p_m [bar]	Intake manifold pressure	T_m [K]	Manifold temperature
α[deg]	Throttle angle	T_a [K]	Ambient temperature
$\dot{m}_{ai}$ [kg/s]	Air mass flow rate into manifold	$\dot{m}_{ao}$ [kg/s]	Air mass flow rate into cylinder
η_{vol}	Volumetric efficiency	N [RPM]	Engine speed
$\dot{m}_f$ [kg/s]	Injected fuel mass flow rate	η_i	Thermal efficiency
τ_f [N · m]	Friction torque	τ_e [N · m]	Effective torque
τ_i [N · m]	Indicated torque	τ_l [N · m]	Load torque

but can describe the major time- varying characteristics. Thus, it can effectively balance the accuracy and complexity of the engine system models. The main engine variables used in the model are given in Table I.

In the following, we will briefly introduce the engine model, which will be used in the subsequent torque estimation. To represent an application example, we model a naturally aspirated port fuel injected engine. We refer to [25], [26] for more details.

A. Air Path Dynamics

For the purpose of modelling, we consider the intake manifold as an adiabatic system, i.e., the pressure and temperature is assumed as constant throughout the manifold. Thus, the pressure variation can be determined based on the ideal gas law and the conservation of mass [25] as

$$\dot{p}_m = \frac{\kappa R}{V_m}\left(\dot{m}_{ai}T_a - \dot{m}_{ao}T_m\right) \tag{1}$$

where V_m is the manifold volume, κ is the ratio of specific heats ($\kappa = 1.4$ for air), and R is the gas constant.

The air mass flow into the manifold, $\dot{m}_{ai}$, is a function of the throttle angle α determined by the driver via the acceleration pedal [25], which is governed by

$$\dot{m}_{ai} = MAX \cdot TC(\alpha) \cdot PRI(p_m) \tag{2}$$

where MAX is a physical constant related to the throttle size; $TC(\alpha)$ is the throttle characteristics depending on the throttle angle α; $PRI(p_m)$ is the pressure ratio influence function of the intake manifold pressure p_m.

The air mass flow rate out of the manifold, $\dot{m}_{ao}$, can be calculated as

$$\dot{m}_{ao} = \sqrt{\frac{T_m}{T_a}}\frac{V_d\eta_{vol}}{120RT_m}Np_m \tag{3}$$

where V_d is the engine displacement, η_{vol} is the volumetric efficiency which depends on the engine speed N.

B. Fuel Path Dynamics

The fuel mass flow rate $\dot{m}_f$ injected into the cylinder is controlled to regulate the air-fuel equivalence ratio λ at the desired value. Therefore, we have

$$\dot{m}_f = \frac{\dot{m}_{ao}}{\lambda L_{th}} \tag{4}$$

where L_{th} is the stoichiometric value (e.g., $L_{th} = 14.7$ for petrol engines).

C. Torque Production Dynamics

The combustion of the air-fuel mixture generates the indicated torque τ_i, which is a function of the engine speed N and the fuel mass flow rate $\dot{m}_f$ as

$$\tau_i = \frac{H_u\eta_i\dot{m}_f}{2\pi N/60} \tag{5}$$

where H_u is the fuel energy constant and the thermal efficiency η_i is exponentially dependent on the engine speed N as in [17] and [26]. Thus, the indicated torque τ_i can be taken as a function of the engine speed N and air mass flow rate $\dot{m}_{ai}$ based on (1)–(5), and denoted as $\tau_i(N, \dot{m}_{ai})$.

The friction dissipation τ_f is mainly determined by the engine speed N as [26]

$$\tau_f(N) = a_0 + a_1N + a_2N^2 \tag{6}$$

where a_0 accounts for the static friction, a_1N represents the hydrodynamic or viscous frictions, a_2N^2 denotes the turbulent dissipation.

Then, the effective engine torque τ_e can be written as

$$\tau_e = \tau_i(N, \dot{m}_{ai}) - \tau_f(N) = f(N, \dot{m}_{ai}) \tag{7}$$

where τ_e can be taken as a lumped function $f(\cdot)$ of the engine speed N and air mass flow rate $\dot{m}_{ai}$.

D. Crankshaft Dynamics

The crankshaft dynamics can be easily modelled using Newton's second law as

$$J\dot{N} = \tau_e - \tau_l \tag{8}$$

where J is the scaled moment of inertia of the engine, τ_l is the load torque. These dynamics together with the torque model (7) are the basis to the estimation schemes in this paper, which are generic to SI and CI engines.

It is noted that the torque production in (5)–(7) is also weakly dependent on the manifold pressure p_m, the spark advance θ_{SA} and the air-fuel ratio λ. The resultant error due to the neglected effect of such factors can be taken as the modeling uncertainties or sensor noise as [17]. Simulation and practical results will show this is valid over fairly large engine transient operating conditions.

E. Problem Statement

The problem to be addressed is to estimate the effective engine torque τ_e by using easily measured variables, e.g., engine speed, air mass flow rate. Considering the previous engine model, it is straightforward to calculate τ_e either from the torque model (7) or from the crankshaft dynamics (8). However, such calculations rely on the knowledge of the engine dynamics and parameters. For (7), $\tau_i(N, \dot{m}_{ai})$ and $\tau_f(N)$ cannot be exactly known for commercial engines due to the nonlinearities and unknown coefficients involved in (5) and (6). For (8), it is difficult to obtain the engine acceleration $\dot{N}$ although one may argue that $\dot{N}$ can be calculated by directly differentiating the engine speed N. However, the performance of such differentiation approximations can be very poor due to sensor noise. Moreover, in these direct calculation methods, the uncertainties would inevitably lead to estimation error, especially when the engine is running in highly time-varying conditions.

To address above issues, there has been a number of publications [2]–[10], which have been proposed by exploiting various observers, where different variables are assumed to be measurable or cascaded observers [17] should be used. This may limit their applicability in practice. This fact drives the motivation of developing simple yet efficient estimators, which uses easily accessed variables (e.g., engine speed N, and air mass flow rate $\dot{m}_{ai}$) with commercial sensors equipped in cars, and avoids noisy sensitive calculations (e.g., differentiation of N).

In this paper, we first estimate the effective torque from the crankshaft dynamics (8) by introducing a new unknown input observer. Moreover, since the function $f(N, \dot{m}_{ai})$ in (7) can be further formulated as a parameterized form with unknown time-varying parameters associated with $\dot{m}_{ai}$ and N, we can also estimate the torque τ_e by investigating novel adaptive laws for estimating time-varying parameters. In these two approaches, we only use the engine speed N and air mass flow rate $\dot{m}_{ai}$, which can be easily measured via standard sensors configured in commercial cars.

III. Unknown Input Observer for Torque Estimation

This section first presents theoretical developments of a new unknown input observer to estimate the effective engine torque τ_e based on (8). We also compare it with two other methods: a sliding mode estimator and a dirty differentiation estimator. In this case, we only use the moment of inertia J, the measured engine speed N and the load τ_l.

A. Unknown Input Observer Design

From the crankshaft model (8), the effective torque τ_e is taken as the unknown 'input'. Thus, the principle of unknown input observer [18] can be further revisited. In this case, we assume the derivative of τ_e is bounded by $\sup_{t\geq 0}|\dot{\tau}_e| \leq \hbar$ for a constant $\hbar > 0$. This assumption has been widely used [23], which is practically feasible for engine applications.

We first define the filtered variables N_f and τ_{lf} with respect to N and τ_l as

$$\begin{cases} k\dot{N}_f + N_f = N, & N_f(0) = 0 \\ k\dot{\tau}_{lf} + \tau_{lf} = \tau_l, & \tau_{lf}(0) = 0 \end{cases} \tag{9}$$

where $k > 0$ is a filter parameter.

Then an ideal invariant manifold [27] is constructed, which will be used to design the unknown input observer.

Lemma 1: Consider the crankshaft model (8) and the filter operation (9), the manifold variable

$$\beta = \frac{J}{k}(N - N_f) + \tau_{lf} - \tau_e \tag{10}$$

is bounded and decreases exponentially for any finite $k > 0$. Moreover, we have

$$\lim_{k\to 0}\left[\lim_{t\to\infty} J(N - N_f)/k + \tau_{lf} - \tau_e\right] = 0 \tag{11}$$

Thus, $\beta = 0$ is an invariant manifold for any $k > 0$.

Proof: The derivative of β with respect to time t is calculated from (9) and (10) as

$$\dot{\beta} = \frac{J\left(\dot{N} - \dot{N}_f\right)}{k} + \dot{\tau}_{lf} - \dot{\tau}_e = -\frac{1}{k}\left(\beta + k\dot{\tau}_e\right) \tag{12}$$

We first prove the boundedness of β. Select a Lyapunov function as $V_\beta = \beta^2/2$, such that

$$\begin{aligned} \dot{V}_\beta &= -\frac{1}{k}\beta\beta - \beta\dot{\tau}_e \leq -\frac{1}{k}\beta^2 + \frac{1}{2k}\beta^2 + \frac{k}{2}\dot{\tau}_e^2 \\ &\leq -\frac{1}{k}V_\beta + \frac{k}{2}\hbar^2 \end{aligned} \tag{13}$$

By solving the inequality (13), one can easily verify that $V_\beta(t) \leq e^{-t/k}V_\beta(0) + k^2\hbar^2/2$. Thus, $\beta(t)$ will exponentially converge to a small compact set bounded by $|\beta(t)| = \sqrt{2V_\beta(t)} \leq \sqrt{\beta^2(0)e^{-t/k} + k^2\hbar^2}$, where its size is determined by the filter parameter k and the upper bound $\hbar$ of $\dot{\tau}_e$, i.e.,$\lim_{t\to\infty}\beta(t) = k\hbar$, which vanishes for sufficiently small k and/or constant torque τ_e (i.e., $\hbar = 0$).

Moreover, for $k \to 0$, it can be verified that $\lim_{k\to 0}[\lim_{t\to\infty}\beta(t)] = 0$, which implies that $\beta(t)$ converges to zero for any bounded $\beta(0)$ and thus $\beta = 0$ is an invariant manifold for $k \to 0$. ◇

It is shown that the above invariant manifold provides a mapping from the variables (N, N_f, τ_{lf}) to the unknown torque τ_e without knowing the angular acceleration $\dot{N}$. Thus, based on the manifold dynamics (10), a feasible estimator of τ_e is

$$\hat{\tau}_e = \frac{J(N - N_f)}{k} + \tau_{lf} \tag{14}$$

Before proving the convergence of estimator (14), we first provide an insight of this estimator. Thus, we apply a low-pass

filter $1/(ks+1)$ on both sides of (8) and have

$$J\dot{N}_f = \tau_{ef} - \tau_{lf} \tag{15}$$

where τ_{ef} is the filtered version of the unknown torque, which is given by

$$k\dot{\tau}_{ef} + \tau_{ef} = \tau_e, \tau_{ef}(0) = 0 \tag{16}$$

On the other hand, from the first equation of (9), we can verify that $(N - N_f)/k = \dot{N}_f$. Then, it follows from (14) and (15) that $\hat{\tau}_e = \tau_{ef}$, which means that the derived estimate is equivalent to the filtered version of the unknown torque. In this case, we can verify that $\dot{\hat{\tau}}_e = \dot{\tau}_{ef} = \frac{1}{k}(\tau_e - \tau_{ef}) = \frac{1}{k}(\tau_e - \hat{\tau}_e)$.

We now define the estimation error as $\tilde{\tau}_e = \tau_e - \hat{\tau}_e$, then the error dynamics are given as

$$\dot{\tilde{\tau}}_e = \dot{\tau}_e - \dot{\hat{\tau}}_e = -\frac{1}{k}\tilde{\tau}_e + \dot{\tau}_e \tag{17}$$

Based on (17), it is clear that the estimation error $\tilde{\tau}_e$ will converge to a small compact set with an arbitrarily faster exponential speed for any small k. Specifically, it can even vanish when the torque τ_e is constant, i.e., $\dot{\tau}_e = 0$. This can be summarized as

Theorem 1: For the crankshaft dynamics (8) with UIO in (14), the estimation error $\tilde{\tau}_e$ exponentially converges to a small set given by the relation $|\tilde{\tau}_e(t)| \leq \sqrt{\tilde{\tau}_e^2(0)e^{-t/k} + k^2\hbar^2}$, so that $\hat{\tau}_e \to \tau_e$ holds for $k \to 0$ or $\hbar \to 0$.

Proof: We select a Lyapunov function $V = \tilde{\tau}_e^2/2$, then calculate its derivative along (17) as

$$\dot{V} = \tilde{\tau}_e\dot{\tilde{\tau}}_e = -\frac{1}{k}\tilde{\tau}_e^2 + \tilde{\tau}_e\dot{\tau}_e \leq -\frac{1}{k}V + \frac{k}{2}\hbar^2 \tag{18}$$

Then, similar to Lemma 1, we can again derive the fact that $|\tilde{\tau}_e(t)| = \sqrt{2V(t)} \leq \sqrt{\tilde{\tau}_e^2(0)e^{-t/k} + k^2\hbar^2}$, which implies that $\tilde{\tau}_e(t) \to 0$ holds for $k \to 0$ and $\hbar \to 0$. ◇

Remark 1: The proposed torque estimator (14) is simple as it only requires the knowledge of the engine inertia J, the engine speed N and load torque τ_l considering the torque production dynamics only. Furthermore, there is only the filter constant k to be tuned, which is set small in practice.

Remark 2: It should be noted that the load torque applied on the engine is known as assumed in [17]. This assumption has been widely used in the literature for torque estimation [4], [17], [24]. In a laboratory, the load torque τ_l can be measured using a dynamometer. In practice, this load torque can be estimated by using a polynomial approximation [32], or considering the vehicle powertrain dynamics [33], [34] but assuming again a further set of parameters and variables to be known. Hence, this increased complexity for online estimation of engine load will not be addressed in this paper due to the limited space.

B. Comparison to Other Methods

In this subsection, we will compare the estimator (14) and two other well-known UIOs as presented in [18] with respect to their convergence property.

1) Sliding Mode Estimator: The sliding mode estimator is based on the principle of the equivalent control [18], [35]. Thus, the following variable structure observer can be constructed

$$J\dot{\hat{N}} = -\tau_l + \lambda_1 \mathrm{sign}(\tilde{\mathrm{N}}) \tag{19}$$

where $\tilde{N} = N - \hat{N}$ is the observer output error and $\lambda_1 > \hbar$ is a positive constant. Then the output error dynamics can be given as

$$J\dot{\tilde{N}} = \tau_e - \lambda_1 \mathrm{sign}(\tilde{\mathrm{N}}) \tag{20}$$

For any $\lambda_1 > |\tau_e|$, it can be proved that $\tilde{N}$ will reach the sliding mode surface $\tilde{N} = 0$ in finite time. Using the notion of the equivalent control [18], [35], we know $\tau_e = \lambda_1 \mathrm{sign}(\tilde{\mathrm{N}})$. However, it is clear that the estimation $\hat{\tau}_e = \lambda_1 \mathrm{sign}(\tilde{\mathrm{N}})$ suffers from the chattering problem due to the use of the signum function $\mathrm{sign}(\tilde{\mathrm{N}})$. To accommodate for this issue and provide a smoother estimator, one can include a low pass filter and propose the following estimator

$$\hat{\tau}_e = \frac{1}{ks+1}\left[\lambda_1 \mathrm{sign}(\tilde{\mathrm{N}})\right] \tag{21}$$

where $\frac{1}{ks+1}[\cdot]$ with bracket $[\cdot]$ in (21) denotes the filter operation of the low pass with transfer function $1/(ks+1)$ applied to the temporal signal $\lambda_1 \mathrm{sign}(\tilde{\mathrm{N}})$.

Then it can be reformulated as

$$\dot{\hat{\tau}}_e = -\frac{1}{k}\hat{\tau}_e + \frac{1}{k}\lambda_1 \mathrm{sign}\left(\tilde{\mathrm{N}}\right) = -\frac{1}{k}\hat{\tau}_e + \frac{1}{k}\tau_e \tag{22}$$

The estimator error $\tilde{\tau}_e = \tau_e - \hat{\tau}_e$ of the sliding mode estimator (21) can be obtained from (22), which is identical to (17). Then, we have:

Lemma 2: For the crankshaft dynamics (8) with sliding mode estimator in (21), the error $\tilde{\tau}_e$ exponentially converges to a set defined by $|\tilde{\tau}_e(t)| \leq \sqrt{\tilde{\tau}_e^2(0)e^{-t/k} + k^2\hbar^2}$, and thus $\hat{\tau}_e \to \tau_e$ holds for $k \to 0$ or $\hbar \to 0$.

Proof: The proof is the same as that of Theorem 1 and thus will not be repeated.

Remark 3: The estimator (21) is designed according to the principle of equivalent control. From (20), the sliding mode observer (19) enforces an invariant manifold $\tilde{N} = 0$ by using discontinuous action $\lambda_1 \mathrm{sign}(\tilde{\mathrm{N}})$ with high-frequency switching. A low-pass filter $1/(ks+1)$ is used in (21) to remedy the chattering phenomenon. However, the bandwidth of this low-pass filter should be set to make a trade-off between the convergence performance of the error $\tilde{\tau}_e$ and the smoothness of $\hat{\tau}_e$. Thus, the constant k in (21) cannot be set arbitrarily small.

2) Dirty Differentiation Estimator: The unknown torque in (8) can also be obtained by using the idea of the so-called 'dirty derivative' [18], where the derivative of N can be approximated by

$$\dot{N} \approx \frac{s}{ks+1}[N] = \frac{N}{k} - \frac{1}{k\,(ks+1)}[N] \tag{23}$$

for a sufficiently small positive constant $k > 0$. Note again the filter operations $\frac{s}{ks+1}[\cdot]$ and $\frac{1}{k(ks+1)}[\cdot]$ are carried out for the temporal signal of N as for (21).

When the derivative $\dot{N}$ in (8) is approximated as (23), the unknown torque τ_e can be estimated as

$$\hat{\tau}_e = \frac{JN}{k} - \frac{J}{k\,(ks+1)}[N] + \tau_l \tag{24}$$

From (8) and (24), we get the estimation error

$$\tilde{\tau}_e = \tau_e - \hat{\tau}_e = \left(Js - \frac{Js}{ks+1}\right)[N] = \frac{Jks^2}{ks+1}[N] \tag{25}$$

This can be represented in the time-domain as

$$\dot{\tilde{\tau}}_e = -\frac{1}{k}\tilde{\tau}_e + J\ddot{N} \tag{26}$$

The analysis for this estimator can be summarized as:

Lemma 3: For the crankshaft dynamics (8) with the estimator in (24), the estimation error $\tilde{\tau}_e$ exponentially converges to a small set defined by $|\tilde{\tau}_e(t)| \le \sqrt{\tilde{\tau}_e^2(0)e^{-t/k} + k^2J^2\bar{\lambda}^2}$ with $\sup_{t\ge 0}|\ddot{N}| \le \bar{\lambda}$, so that $\hat{\tau}_e \to \tau_e$ holds for $k \to 0$ and $\bar{\lambda} \to 0$.

Proof: Select the Lyapunov function as $V = \tilde{\tau}_e^2/2$, then its derivative along (26) can be obtained as

$$\dot{V} = \tilde{\tau}_e\dot{\tilde{\tau}}_e = -\frac{1}{k}\tilde{\tau}_e^2 + \tilde{\tau}_e J\ddot{N} \le -\frac{1}{k}V + \frac{k}{2}J^2\bar{\lambda}^2 \tag{27}$$

Then similar to the proof of Theorem 1, one may obtain $V(t) \le e^{-t/k}V(0) + k^2J^2\bar{\lambda}^2/2$, which implies the estimation error converges to a set in $\tilde{\tau}_e(t)$ given by the inequality $|\tilde{\tau}_e(t)| \le \sqrt{\tilde{\tau}_e^2(0)e^{-t/k} + k^2J^2\bar{\lambda}^2}$. ◇

Remark 4: One may find from Lemma 3 that the estimation error of (24) depends on the upper bound of the second order derivative of the engine speed (e.g., $\sup_{t\ge 0}|\ddot{N}| \le \bar{\lambda}$) and the inertia J. Thus, the estimator (24) may be very sensitive to sensor noise. In contrast, the estimation errors of (14) and (21) depend only on the upper bound of the first order derivative of the unknown input $\dot{\tau}_e$ (e.g., $\sup_{t\ge 0}|\dot{\tau}_e| \le \hbar$). Moreover, one may find that the engine speed N is filtered by a low pass filter in (9) to avoid the derivative approximation in (23). The inclusion of such filters can lead to better convergence response than (24).

IV. Robustness of Unknown Input Observers

In practice, the engine speed N and the load torque τ_l that are used to facilitate the above torque estimators are measured by sensors. Thus, the measurements may contain unavoidable sensor noise. In this section, we will further compare the robustness of the above estimators against measurement noise. In this case, we define w_1, w_2 as the noise signals perturbing the engine speed N and the load torque τ_l, respectively. Then the measured variables used in the torque estimators are

$$\bar{N} = N + w_1, \bar{\tau}_l = \tau_l + w_2 \tag{28}$$

Without loss of generality, we assume that the noise signals are all bounded, i.e., $|w_1| \le \eta_1, |w_2| \le \eta_2, |\dot{w}_1| \le \eta_3, |\dot{w}_2| \le \eta_4$ holds for constants $\eta_1, \eta_2, \eta_3, \eta_4 > 0$.

A. Unknown Input Observer

The estimator (14) with (28) is reformulated as

$$\begin{cases} k\dot{\bar{N}}_f + \bar{N}_f = \bar{N}, & \bar{N}_f(0) = 0 \\ k\dot{\bar{\tau}}_{lf} + \bar{\tau}_{lf} = \bar{\tau}_l, & \bar{\tau}_{lf}(0) = 0 \end{cases} \tag{29}$$

$$\hat{\tau}_e = \frac{J(\bar{N} - \bar{N}_f)}{k} + \bar{\tau}_{lf} \tag{30}$$

From (8) and (28)–(30), one can verify that

$$\hat{\tau}_e = J\dot{\bar{N}}_f + \bar{\tau}_{lf} = J\dot{N}_f + J\dot{w}_{1f} + \tau_{lf} + w_{2f} \tag{31}$$

where $\dot{w}_{1f}$ and w_{2f} are the filtered version of $\dot{w}_1$ and w_2 in terms of the filter $1/(ks+1)$. Then we can further verify the following equation

$$\dot{\hat{\tau}}_e = -\frac{1}{k}\hat{\tau}_e + \frac{1}{k}(J\dot{w}_1 + w_2) + 1/k(J\dot{N} + \tau_l) \tag{32}$$

In this case, the estimation error of (30) can be given as

$$\dot{\tilde{\tau}}_e = -\frac{1}{k}\tilde{\tau}_e + \dot{\tau}_e - \frac{1}{k}(J\dot{w}_1 + w_2) \tag{33}$$

Similar to Theorem 1, we have

Theorem 2: For the crankshaft dynamics (8) with measurement noise w_1, w_2 in the engine speed N and load torque τ_l, then the estimation error of UIO (30) exponentially converges to a set defined by $|\tilde{\tau}_e(t)| \le \sqrt{\tilde{\tau}_e^2(0)e^{-t/k} + k^2[\hbar + (J\eta_3 + \eta_2)/k]^2}$.

Proof: The proof can be conducted by calculating the derivative of Lyapunov function $V = \tilde{\tau}_e^2/2$ along (33). The detailed analysis is similar to that of Theorem 1, and we will not repeat it again. ◇

In the presence of sensor noise w_1, w_2, the convergence property $\hat{\tau}_e \to \tau_e$ does not hold even for $k \to 0$ and $\hbar \to 0$. However, a constant measurement offset of N due to the sensor drifts (i.e., $w_1 = $ const. and $\eta_3 = 0$) can be compensated without knowing the offset magnitude.

B. Sliding Mode Estimator

From (8) and (28), the measured system dynamics can be described as

$$J\dot{\bar{N}} = \tau_e + J\dot{w}_1 - \bar{\tau}_l + w_2 \tag{34}$$

Thus, we can construct a sliding mode observer for (34) by using the measured variable as

$$J\dot{\hat{\bar{N}}} = -\bar{\tau}_l + \lambda_1 \mathrm{sign}(\tilde{\mathrm{N}}) \tag{35}$$

where $\tilde{N} = \bar{N} - \hat{\bar{N}}$ is the observer output error, which can be given as $J\dot{\tilde{N}} = \tau_e + J\dot{w}_1 + w_2 - \lambda_1 \mathrm{sign}(\tilde{\mathrm{N}})$. We can select the observer gain such that $\lambda_1 > |\tau_e| + \eta_2 + J\eta_3$, and then verify that $\tilde{N} = 0$ can be achieved in finite time. In this case, the equivalent control is $\tau_e + J\dot{w}_1 + w_2 = \lambda_1 \mathrm{sign}(\tilde{\mathrm{N}})$.

The estimator error of (21) is modified as

$$\begin{aligned} \tilde{\tau}_e &= \tau_e - \frac{1}{ks+1}[\tau_e + J\dot{w}_1 + w_2] \\ &= \frac{k}{ks+1}[\dot{\tau}_e] - \frac{1}{ks+1}[J\dot{w}_1 + w_2] \end{aligned} \tag{36}$$

which is in the time-domain represented as (33).

Consequently, the convergence property of this sliding mode estimator (21) can be summarized as

Lemma 4: For the crankshaft dynamics (8) with measurement noise w_1, w_2 in the engine speed N and load torque τ_l, the estimation error of estimator (21) with the modified sliding mode observer (35) will converge to a set defined by $|\tilde{\tau}_e(t)| \leq \sqrt{\tilde{\tau}_e^2(0)e^{-t/k} + k^2[\hbar + (J\eta_3 + \eta_2)/k]^2}$.

Proof: The proof is the same as that of Theorem 2 because its error dynamics are the same as (33).

Remark 5: From Theorem 2 and Lemma 4, it is shown that the robustness property of the proposed estimator (14) is comparable to the sliding mode estimator (21). However, in contrast to the sliding mode estimator (21), the proposed estimator (14) does not employ a switching element, i.e., it does not have the chattering problem, and thus it provides a smooth response even for small k.

C. Dirty Differentiation Estimator

When there are sensor noise signals w_1, w_2 in the engine speed N and load torque τ_l, the estimator (24) can be reformulated as follows

$$\hat{\tau}_e = \frac{J\bar{N}}{k} - \frac{J}{k\,(ks+1)}[\bar{N}] + \bar{\tau}_l \tag{37}$$

which equals to

$$\hat{\tau}_e = \frac{Js}{ks+1}[N] + \frac{Js}{ks+1}[w_1] + \tau_l + w_2 \tag{38}$$

Consequently, the estimation error of (37) is obtained as

$$\tilde{\tau}_e = \left(Js - \frac{Js}{ks+1}\right)[N] = \frac{Jks^2}{ks+1}[N] - \frac{Js}{ks+1}[w_1] - w_2 \tag{39}$$

To facilitate the convergence analysis, the error (39) is further represented as

$$\dot{\tilde{\tau}}_e = -\frac{1}{k}\tilde{\tau}_e + J\ddot{N} - \dot{w}_2 - \frac{1}{k}(w_2 + J\dot{w}_1) \tag{40}$$

Then we can prove the following lemma, which summarize the convergence property of estimator (37).

Lemma 5: For the crankshaft dynamics (8) with measurement noise w_1, w_2 in the engine speed N and load torque τ_l, the estimation error of (37) converges to a set defined by $|\tilde{\tau}_e(t)| \leq \sqrt{\tilde{\tau}_e^2(0)e^{-t/k} + k^2[J\bar{\lambda} + \eta_4 + (J\eta_3 + \eta_2)/k]^2}$.

As shown in Lemma 5, the ultimate bound of the estimation error of the dirty differentiation estimator (37) depends on also the upper bound $|\dot{w}_2| \leq \eta_4$, which defines the magnitude of the derivative $\dot{w}_2$. Consequently, the estimator (37) is more sensitive to sensor noise than the other two estimators. This will be verified in the simulations and experiments.

D. Comparative Discussion

From the above analysis, we have the following observations:

1) The estimation error of the proposed UIO (14) is comparable to that of the sliding mode observer (21), even in the presence of measurement noise. In fact, theoretical analysis indicate that the convergence and robustness of them are the same. However, the sliding mode observer (21) suffers from the well-known chattering issue, which leads to non-smooth estimation response, while the suggested UIO (14) can provide smooth estimation response.
2) The estimation error of the dirty differentiation estimator (24) depends on the second order derivative of the engine speed $\ddot{N}$, which can be very large in the dynamic engine scenarios. Moreover, it is also sensitive to sensor noise in comparison to other methods, i.e., high-frequency noise may deteriorate its performance.
3) In terms of parameter tuning, the proposed UIO (14) and the dirty differentiation estimator (24) have only one constant (e.g., $k > 0$) to be selected by the designers. This filter coefficient can be set small to allow for higher bandwidth of the low-pass filter (9). However, the response of the derivative approximation in (23) will show significant oscillations when k is too small, in contrast to the UIO (14).
4) The sliding mode estimator (21) needs to set the observer gain $\lambda_1 > |\tau_e|$, which depends on the knowledge of the upper bound of the torque. Moreover, the requirement for the smoothness of the sliding mode estimator (21) does not allow a too small $k > 0$.

TABLE II
COMPARISONS OF THREE ESTIMATORS

Methods	Ultimate error bound	Chattering	Noise sensitivity
UIO	$\sup_{t\geq 0}\|\tilde{\tau}_e\| \leq \hbar$	No	$\dot{w}_1, w_2$
Sliding mode	$\sup_{t\geq 0}\|\tilde{\tau}_e\| \leq \hbar$	Yes	$\dot{w}_1, w_2$
Dirty differentiation	$\sup_{t\geq 0}\|\ddot{N}\| \leq \bar{\lambda}$	No	$\dot{w}_1, w_2, \dot{w}_2$

The convergence, the robustness property and key features of these three estimators can be summarized in Table II.

V. Adaptive Time-Varying Parameter Estimation

In Section III, we take the unknown effective engine torque τ_e as an unknown input (time-varying signal) of crankshaft dynamics (8), and then solve the torque estimation problem via the principle of UIO. However, the estimation of this effective engine torque can be significantly facilitated if other engine dynamics associated with measurable data are considered. In this section, we will study the engine torque estimation problem from another perspective: time-varying parameter estimation. This method will facilitate a deeper understanding of the engine dynamics. Moreover, the theoretical developments to be presented also provide a feasible method for the estimation of time-varying parameters for other applications. It is noted that adaptive parameter estimation for time-varying parameters has not been fully solved in the field [20].

Thus, we revisit the torque model (7) and find that the effective torque τ_e can be taken as a function of the engine speed N and the air mass flow rate $\dot{m}_{ai}$, which has been also used in [4],

[10], and [17]. Hence, we can present (8) in a parameterized form with time-varying parameters

$$J\dot{N} = f(N, \dot{m}_{ai}) - \tau_l = [N\ \dot{m}_{ai}] \begin{bmatrix} \theta_1(t) \\ \theta_2(t) \end{bmatrix} - \tau_l + \delta$$
$$= \Phi\Theta(t) - \tau_l + \delta \tag{41}$$

where $\Phi = [N\ \dot{m}_{ai}]$ is the known regressor vector. $\Theta(t) = [\theta_1(t)\ \theta_2(t)]^T$ is the unknown vector to be estimated, which contains time-varying parameters, and δ defines the effect of bounded disturbances or approximation errors. The problem of estimating the effective torque $\tau_e = \Phi\Theta(t)$ can be achieved provided that the time-varying parameters $\Theta(t)$ can be precisely estimated. It is assumed in this section that the derivative of $\Theta(t)$ with respect to time t is bounded by $\|\dot{\Theta}(t)\| \leq \varpi$ for a positive constant $\varpi > 0$.

For a linearly parameterized system (41), if the unknown parameters are constant, i.e., $\Theta = \text{const.}$, the gradient descent algorithms [21] can be used. However, as pointed out in [20], the ability of the gradient method to track time-varying parameters and their robustness are limited. In this section, we will propose a new parameter estimation scheme by further exploiting the parameter estimation error based adaptation algorithm in [28] and [29].

We define the filtered variables N_f,τ_{lf} in (9) and Φ_f as

$$k\dot{\Phi}_f + \Phi_f = \Phi,\ \Phi_f(0) = 0 \tag{42}$$

where $k > 0$ is the same constant as in (9).

Then similar to Lemma 1 in Section III, an ideal invariant manifold [27] can be constructed, such that

Lemma 6: Consider system (41) with filters (9) and (42), then the manifold variable $\beta = [J(N - N_f)/k + \tau_{lf} - \Phi_f\Theta(t)]$ is bounded for any finite $k > 0$. Moreover, the manifold $\lim_{k\to 0}[(N - N_f)J/k + \tau_{lf} - \Phi_f\Theta(t)] = 0$ is invariant for $\delta = 0$.

Proof: The detailed proof is similar to that of Lemma 1. ◇

The manifold variable $\beta = [(N - N_f)J/k + \tau_{lf} - \Phi_f\Theta(t)]$ is independent of the engine speed derivative $\dot{N}$. Moreover, it provides an implicit information of the unknown parameter $\Theta(t)$ with available variables $(N, N_f, \tau_{lf}, \Phi_f)$. To further show this fact for any finite $k > 0$, we apply a filter $1/(ks + 1)$ on both sides of (41), then

$$\frac{Js}{ks+1}[N] = \frac{1}{ks+1}[\Phi\Theta(t)] - \frac{1}{ks+1}[\tau_l] + \frac{1}{ks+1}[\delta] \tag{43}$$

Consider the first equation of (9) and the Swapping Lemma [21] for the term $\frac{1}{ks+1}[\Phi\Theta(t)]$, we rewrite (43) as

$$\frac{J\,(N - N_f)}{k} = -\tau_{lf} + \Phi_f\Theta(t) - \zeta \tag{44}$$

where the residual term $\zeta = \frac{k}{ks+1}[\Phi_f\dot{\Theta}] + \delta_f$ comes from the filtering operation of error δ and $\Phi\Theta(t)$ when the parameter $\Theta(t)$ is time-varying. For $\Theta = \text{const.}$ and $\delta = 0$, we have $\zeta = 0$.

Since Φ is bounded in engine systems, its filtered version Φ_f is also bounded, i.e., $\|\Phi_f\| \leq \mu$ for a constant $\mu > 0$. This together with the fact $\|\Theta(t)\| \leq \varpi$ implies that ζ is bounded for any $k > 0$, (i.e., $|\zeta| \leq \gamma$ for a positive constant γ). In this case, ζ can be considered as a 'disturbance' perturbing the ideal manifold in Lemma 6.

Thus, we define the auxiliary variables P, Q as

$$\begin{cases} \dot{P} = -\ell P + \Phi_f^T\Phi_f, & P(0) = 0 \\ \dot{Q} = -\ell Q + \Phi_f^T\left[J(N - N_f)/k + \tau_{lf}\right], & Q(0) = 0 \end{cases} \tag{45}$$

where $\ell > 0$ is another positive constant serving as the forgetting factor to retain the boundedness of P and Q.

Then by using P and Q, we can further define vectors W_1 and W_2 as

$$W_1 = P\hat{\Theta} - Q \tag{46}$$

$$W_2 = \Phi_f^T\Phi_f\hat{\Theta}(t) - \Phi_f^T\left[J(N - N_f)/k + \tau_{lf}\right] \tag{47}$$

where $\hat{\Theta}(t)$ is the estimate of $\Theta(t)$, which will be online updated by the following adaptive laws.

We define $\lambda_{\max}(\cdot), \lambda_{\min}(\cdot)$ as the maximum and minimum eigenvalues of the corresponding matrices and first prove the following facts:

Lemma 7: The variables in (46) and (47) are equivalent to

$$W_1 = -P\tilde{\Theta} + \psi \tag{48}$$

$$W_2 = -\Phi_f^T\Phi_f\tilde{\Theta} + \Phi_f^T\zeta \tag{49}$$

where $\psi = \int_0^t e^{-\ell(t-\tau)}\Phi_f^T(\tau)\zeta(\tau)d\tau$ is a bounded residual error satisfying $\|\psi\| \leq \|\Phi_f\||\zeta|/\ell = \mu\gamma/\ell$, and $\tilde{\Theta} = \Theta - \hat{\Theta}$ is the estimation error.

Proof: The proof can be carried out by solving the matrix equation (45), and substituting (44) into (46), (47). ◇

Lemma 8: [28], [29]: The matrix P defined in (45) is positive definite (i.e., $\lambda_{\min}(P) > \sigma_1 > 0$) provided that the regressor matrix Φ in (41) is Persistently Excited (PE), i.e., $\int_t^{t+T}\Phi(\tau)\Phi^T(\tau)d\tau \geq \varepsilon I, \forall t \geq 0$ for $T > 0,\ \varepsilon > 0$.

Proof: Please refer to our previous work [28], [29] for a similar proof. ◇

As indicated in Lemma 7, we can find that the variables $W_1,\ W_2$ derived from the measured engine variables are measures of the estimation error $\tilde{\Theta}$, in particular when $\zeta = 0$. Thus, as from our previous work [28], [29], they can be used to drive adaptive laws with guaranteed convergence. In particular W_2 is suited to estimate time-varying parameters, as demonstrated in the next section.

A. Constant Learning Gain

The following adaptive law is first designed to online update $\hat{\Theta}$ as

$$\dot{\hat{\Theta}} = -\Gamma(W_1 + \kappa W_2) \tag{50}$$

where $\Gamma > 0$ is a constant gain, and $\kappa > 0$ is a constant chosen to trade-off the performance and robustness.

Theorem 3: Consider the engine crankshaft dynamics (41) with unknown parameter Θ and the adaptive law (50). When Φ is PE, then $\tilde{\Theta}$ converges to a compact set $\Omega =$

$\{\tilde{\Theta}|\|\tilde{\Theta}\| \le \sqrt{\frac{[m\mu^2\gamma^2(\kappa^2+1/\ell^2)+m\varpi^2/\lambda^2_{\min}(\Gamma)]\lambda_{\max}(\Gamma^{-1})}{2(\sigma_1-3/2m)\lambda_{\min}(\Gamma^{-1})}}\}$, and the engine torque estimate can be obtained as $\hat{\tau}_e = \Phi\hat{\Theta}$.

Proof: We select a Lyapunov function as $V = \tilde{\Theta}^T\Gamma^{-1}\tilde{\Theta}/2$ and use Young's inequality $a^Tb \le a^Ta/2m + mb^Tb/2$ for any constant $m > 0$, and then can calculate $\dot{V}$ along (50) with (48) and (49) as

$$\begin{aligned}\dot{V} &= -\tilde{\Theta}^T P\tilde{\Theta} + \tilde{\Theta}^T\psi - \kappa\tilde{\Theta}^T\Phi_f^T\Phi_f\tilde{\Theta} + \kappa\tilde{\Theta}^T\Phi_f^T\zeta + \tilde{\Theta}^T\Gamma^{-1}\dot{\Theta} \\ &\le -(\sigma_1 - \frac{3}{2m})\left\|\tilde{\Theta}\right\|^2 + \frac{m\mu^2\gamma^2}{2\ell^2} + \frac{m\mu^2\gamma^2\kappa^2}{2} + \frac{m\varpi^2}{2\lambda^2_{\min}(\Gamma)} \\ &\le -\alpha V + \rho \end{aligned} \tag{51}$$

where $\alpha = 2(\sigma_1 - 3/2m)/\lambda_{\max}(\Gamma^{-1})$, $\rho = m\mu^2\gamma^2(\kappa^2 + 1/\ell^2)/2 + m\varpi^2/2\lambda^2_{\min}(\Gamma)$ are all positive when the parameter is set as $m \ge 3/2\sigma_1$. Then, the solution of (51) is $V(t) \le e^{-\alpha t}V(0) + \rho/\alpha$, which implies

$$\begin{aligned}\|\tilde{\Theta}\| &\le \sqrt{2V(t)/\lambda_{\min}(\Gamma^{-1})} \\ &\le \sqrt{[\|\tilde{\Theta}(0)\|^2\lambda_{max}(\Gamma^{-1})e^{-\alpha t} + 2\rho/\alpha]/\lambda_{\min}(\Gamma^{-1})}.\end{aligned}$$

Thus, the estimation error $\tilde{\Theta}$ exponentially converges to a compact set defined in Theorem 2, whose size is determined by the excitation level (e.g., σ_1), the residual error γ due to variations of parameters and the adaptive gain Γ. The convergence rate α depends on the persistent excitation level σ_1 and the learning gain Γ. ◇

Remark 6: Note the matrix P in (45) and (48) versus the regressor matrix $\Phi_f^T\Phi_f$ in (49). Hence, P represents the (averaged) data history of the instant information $\Phi_f^T\Phi_f$. P is invertible once the regressor Φ is PE (Lemma 8). Hence, W_1 is also a filtered version of W_2 by applying $1/(s+\ell)$ in (49). This again introduces an 'averaging' effect and improves the robustness of the adaptive laws. W_1 is essential to estimator convergence and robustness. However, the 'averaging' effect may reduce the ability to track fast time-varying parameters. (The influence of a similar 'averaging operator' was discussed in [20] for the least-squares algorithm). On the other hand, the variable W_2 contains the instant error information which can help to estimate fast time-varying dynamics, while it may be sensitive to noise. In this respect, the constant κ is chosen as a tradeoff between performance and robustness.

Remark 7: As shown in Lemma 7, a large filter parameter ℓ can reduce the amplitude of the residual error ψ, while too large ℓ may introduce a dc gain $1/\ell$ in (45) and decrease the amplitude of P; thus a large ℓ may reduce the convergence speed of the adaptive law (50). Thus, the parameter ℓ cannot be set too large in practice.

Remark 8: It should be noted that the proposed adaptive law (50) can be directly used for estimating unknown constant parameter Θ (i.e., $\dot{\Theta} = 0$). In this case, we know that $\zeta = \psi = 0$ is true, such that the estimation error of the adaptive law (50) will exponentially converge to zero.

B. Time-Varying Learning Gain

It is shown that the estimation error $\tilde{\Theta}$ in (48) and (49) is associated with the time-varying regressor Φ_f for the matrices P in (48) and $\Phi_f^T\Phi_f$ in (49), respectively. The involvement of such dynamics in the adaptive law (50) may not be desirable, because the error convergence speed of (50) increases for large regressor $\Phi_f^T\Phi_f$ and P, while the amplitude of residual terms ψ and $\Phi_f^T\zeta$ in W_1, W_2 also increases for large regressor Φ_f, and thus leads to a large error bound defined in Theorem 3. This contradictory effect of P in (48) and $\Phi_f^T\Phi_f$ in (49) can be compensated so that the estimation response can be improved. Inspired by the Least-squares algorithm, we introduce a time-varying adaptive gain to compensate for the effects of P and $\Phi_f^T\Phi_f$ in (50). We now derive another matrix K as follows

$$\dot{K} = \ell K - K\Phi_f^T\Phi_f K, \quad K^{-1}(0) = K_0 > 0 \tag{52}$$

Then based on the equality $\frac{d}{dt}KK^{-1} = \dot{K}K^{-1} + K\frac{d}{dt}K^{-1} = 0$, one can obtain

$$\begin{aligned}K &= [e^{-\ell t}K_0 + \int_0^t e^{-\ell(t-\tau)}\Phi_f^T(\tau)\Phi_f(\tau)d\tau]^{-1} \\ &= [e^{-\ell t}K_0 + P]^{-1}\end{aligned} \tag{53}$$

From (53), we can find that the matrix K exponentially converges to the inverse of P, i.e., $K \cdot P \to I$. Consequently, we can use K as an adaptive learning gain to eliminate the effect of P in the adaptive law. This provides a modified adaptive law

$$\dot{\hat{\Theta}} = -\Gamma K(W_1 + \kappa W_2) \tag{54}$$

where $\Gamma > 0$ is a constant and K is the time-varying matrix which is online updated based on (52).

Before presenting the main results of this section, we first analyze the boundedness of K based on (53) as

$$K^{-1}(t) = e^{-\ell t}K^{-1}(0) + \int_0^t e^{-\ell(t-\tau)}\Phi_f^T(\tau)\Phi_f(\tau)d\tau \tag{55}$$

Considering the PE condition $\int_t^{t+T}\Phi(\tau)\Phi^T(\tau)d\tau \ge \varepsilon I$, one can verify for $t > T > 0$ the following inequality

$$\begin{aligned}K^{-1}(t) &\ge \int_0^t e^{-\ell(t-\tau)}\Phi_f^T(\tau)\Phi_f(\tau)d\tau \\ &\ge \int_{t-T}^t e^{-\ell(t-\tau)}\Phi_f^T(\tau)\Phi_f(\tau)d\tau \ge e^{-\ell T}\varepsilon I\end{aligned} \tag{56}$$

On the other hand, for any bounded regressor $\|\Phi_f\| \le \mu$, one can also verify from (53) that

$$K^{-1}(t) \le K^{-1}(0) + \mu^2\int_0^t e^{-\ell(t-\tau)}d\tau \le K_0 + \mu^2 I \tag{57}$$

Consequently, it follows from (56) and (57) that

$$\gamma_1 I \le K(t) \le \gamma_2 I \tag{58}$$

for constants $\gamma_1 = 1/(\lambda_{\min}(K_0) + \mu^2)$ and $\gamma_2 = e^{\ell T}/\varepsilon$.

Now, the main results of this subsection can be given as:

Theorem 4: For engine crankshaft dynamics (41) with unknown parameter Θ, the adaptive law (54) is used when Φ is PE, then $\tilde{\Theta}$ converges to a compact set defined by $\|\tilde{\Theta}\| \leq \sqrt{\frac{\gamma_2[m\mu^2\gamma^2(\kappa^2+1/\ell^2)+m\varpi^2/\gamma_1^2\Gamma^2]}{\gamma_1(2\sigma_1+\ell/\gamma_2\Gamma-\mu^2/\Gamma-3/m)}}$, and the engine torque can be obtained as $\hat{\tau}_e = \Phi\hat{\Theta}$.

Proof: We select a Lyapunov function as $V = \tilde{\Theta}^T K^{-1}\tilde{\Theta}/2\Gamma$, then its derivative $\dot{V}$ is calculated along (52) and (54) as

$$\begin{aligned}\dot{V} =& \frac{1}{\Gamma}\tilde{\Theta}^T K^{-1}\dot{\tilde{\Theta}} + \frac{1}{2\Gamma}\tilde{\Theta}^T \dot{K}^{-1}\tilde{\Theta} = \frac{1}{\Gamma}\tilde{\Theta}^T K^{-1}\dot{\Theta} - \tilde{\Theta}^T P\tilde{\Theta} + \tilde{\Theta}^T\psi \\ & - \kappa\tilde{\Theta}^T\Phi_f^T\Phi_f\tilde{\Theta} + \kappa\tilde{\Theta}^T\Phi_f^T\zeta + \frac{1}{2\Gamma}\tilde{\Theta}^T(-\ell K^{-1} + \Phi_f^T\Phi_f)\tilde{\Theta} \\ \leq & -(\sigma_1 + \ell/2\gamma_2\Gamma - \mu^2/2\Gamma - 3/2m)\left\|\tilde{\Theta}\right\|^2 \\ & + \frac{m\mu^2\gamma^2}{2\ell^2} + \frac{m\mu^2\gamma^2\kappa^2}{2} + \frac{m\varpi^2}{2\gamma_1^2\Gamma^2} \\ \leq & -2\Gamma\gamma_1(\sigma_1 + \ell/2\gamma_2\Gamma - \mu^2/2\Gamma - 3/2m)V \\ & + \frac{m\mu^2\gamma^2}{2\ell^2} + \frac{m\mu^2\gamma^2\kappa^2}{2} + \frac{m\varpi^2}{2\gamma_1^2\Gamma^2} \end{aligned} \tag{59}$$

where $m > 0$ is a constant which has been used for Young's inequality similar to Theorem 3. Then as for the analysis in the proof of Theorem 3, the ultimate bound of the estimation error shown in Theorem 4 can be calculated from (59). The convergence rate here depends stronger on Γ. Hence, compared to Theorem 3, it is noted that the learning gain Γ can be chosen as a larger constant to reduce the error bound and to increase convergence. ◇

Remark 9: Lemma 8 provides an intuitive method to online validate the PE condition of regressor Φ by calculating the minimum eigenvalue of P and test for $\lambda_{\min}(P) > \sigma_1 > 0$ as [28] and [29]. This PE condition is used to prove the convergence for adaptive laws [30].

VI. Simulation

In this section, we first validate the proposed estimation methods by using a dynamic simulator, which was built in a commercial engine simulation software GT-Power (Ricardo Wave) based on a well calibrated engine model.

A. GT-Power Model

The engine model is a commercially available benchmark simulation model in GT-Power [31], which is based on a turbocharged 2.0 L four-cylinder SI engine with direct injection. It is well calibrated from geometry measurements (valves, pipes, cylinders etc.) and practical experiments. We predefine the engine speed profile, and then the throttle angle is driven by a feedback controller to cope with the load demand. In comparison to the MVEM used in [24], the GT power model can simulate more realistic engine characteristics because the thermal mechanics and the emission dynamics can be more accurately modelled [31].

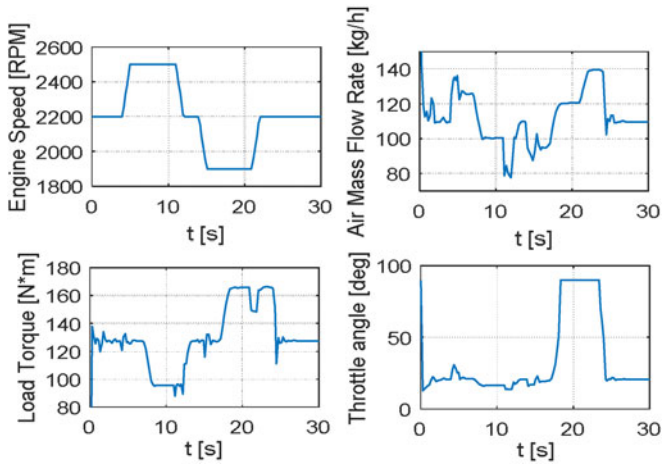

Fig. 2. The engine dynamics of the GT-Power model.

B. Simulation Results

By using a speed feedback controller, the engine model runs from acceleration to deceleration, i.e., $N = 2200 \rightarrow 2500 \rightarrow 2200 \rightarrow 1900$ [RPM] at $t = 0,\ 4,\ 12$ and 14 [s] to test the transient response covering a relatively wider engine operation regime. Thus, both the transient and steady-state response of the engine model can be shown in Fig. 2, where the throttle angle, the engine speed, the air mass flow rate and the load torque are provided.

For fair comparison, the following performance indices are used to evaluate the estimation error $\tilde{\tau}_e$ response.

1) Integrated Squared Error (ISE)

$$ISE = \int \tilde{\tau}_e^2(t)dt \tag{60}$$

2) Maximum Absolute Error (MAE)

$$MAE = \max\{|\tilde{\tau}_e(t)|\} \tag{61}$$

3) Standard Deviation (SD)

$$SD = \sqrt{\frac{1}{T}\int [\tilde{\tau}_e(t) - \mu_e]^2 dt} \tag{62}$$

where μ_e is the average error. It is noted that the above performance indices have been widely used to characterize the error performance [37], [38]. The MAE is a temporal worst case of the absolute estimation error, while SD can quantify the variation or dispersion of a set of data values. These performance indices are not necessarily valid for time-invariance cases only.

We first test the three unknown torque estimators presented in Section III. The proposed UIO (14) is compared with the sliding mode estimator (21) and the dirty differentiation estimator (24) with $k = 0.01$ and $\lambda_1 = 150$, and zero initial condition. In order to validate the robustness of these estimators, random noise $w_1 = N(0, 20)$ and $w_2 = N(0, 20)$ are added to the measured engine speed N and load torque τ_l. Fig. 3 shows the torque estimation performance of these three different methods. The corresponding torque estimation errors are presented in Fig. 4. It is found from Figs. 3 and 4 that the proposed UIO (14) achieves

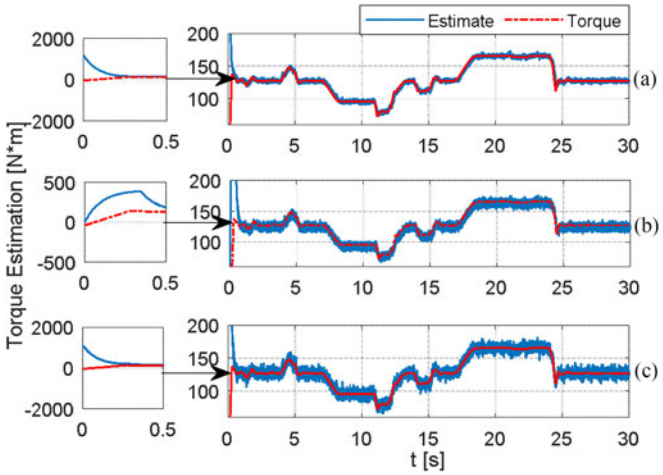

Fig. 3. Torque estimation with different methods. (a) UIO (14). (b) Sliding mode estimator (21). (c) Dirty differentiation estimator (24).

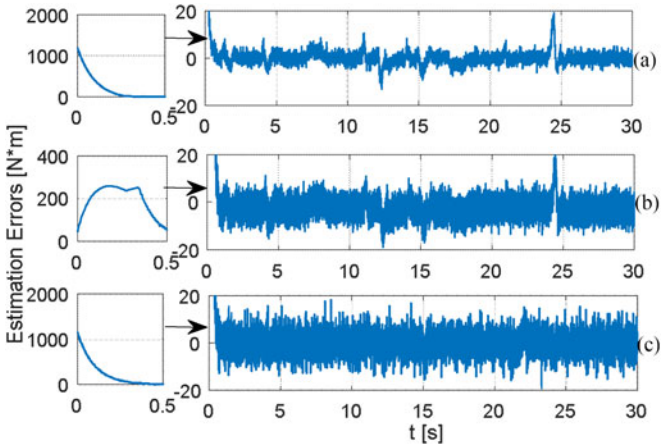

Fig. 4. Torque estimation errors with different methods. (a) UIO (14). (b) Sliding mode estimator (21). (c) Dirty differentiation estimator (24).

TABLE III
TORQUE ESTIMATION PERFORMANCE INDICES

Index	UIO	Sliding mode	Dirty differentiation
ISE	3.5653e + 4	1.3739e + 5	1.0814e + 5
MAE	19.0230	20.4237	18.9628
SD	2.8135	4.9259	4.9015

a better response than (21) and (24) in terms of both transient and steady-state response. This is because the sliding mode estimator (21) has the unavoidable chattering phenomenon and thus leads to oscillations in the estimated torque. Moreover, the estimator (24) is sensitive to the sensor noise, where the estimation error bound is affected by the upper bound of the second order derivative of the engine speed, i.e., $\ddot{N}$, as illustrated in Lemma 5.

These observations can also be illustrated by using the above three performance indices, which are calculated using the data point from 5s to 30s. The indices are shown in Table III. The ISE and SD of (14) is much less than the others. However, it is noted that the MAE of the estimator (24) is slightly smaller

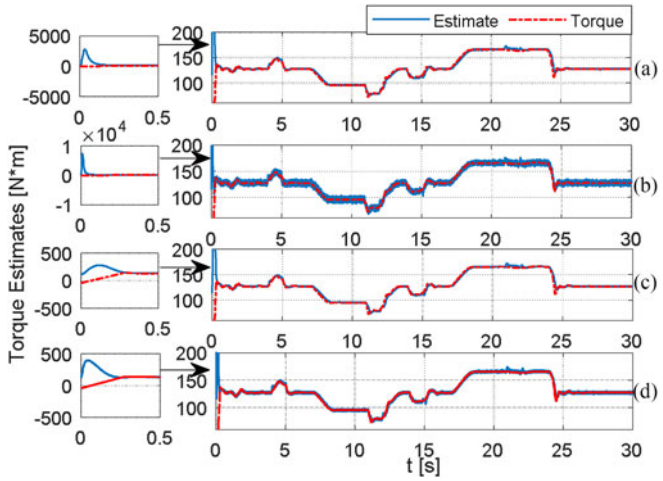

Fig. 5. Torque estimation with: (a) adaptive law (50) with $\kappa = 0$, (b) adaptive law (50) with $\kappa = 0.1$, (c) adaptive law (54) with $\kappa = 0$, and (d) adaptive law (54) with $\kappa = 0.1$.

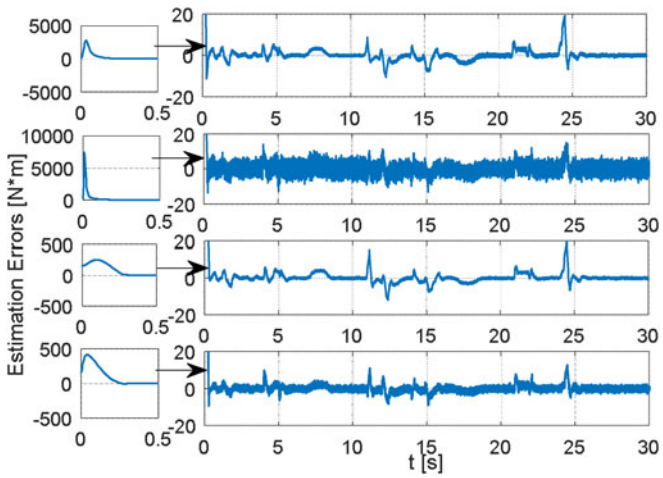

Fig. 6. Torque estimation errors with: (a) adaptive law (50) with $\kappa = 0$, (b) adaptive law (50) with $\kappa = 0.1$, (c) adaptive law (54) with $\kappa = 0$, and (d) adaptive law (54) with $\kappa = 0.1$.

than that of (14). This can be explained by the fast convergence of (24) at transients in spite of its poor robustness to noise.

We further test the adaptive time-varying parameter methods from Section V, i.e., the adaptive law (50) with constant learning gain and the adaptive law (54) with time-varying learning gain. The parameters in (42) and (45) are $k = 0.01$, $\ell = 10$ and $\Gamma = diag[0.1100]$ for (50) with zero initial condition $\hat{\Theta}(0) = 0$. Again, the same random noise signals are added to test the robustness of these adaptations. The adaptive laws (50) and (54) are verified with $\kappa = 0$ and $\kappa = 0.1$, respectively; in the second case, the instant information in W_2 is used together with W_1, which is dedicated to improve transient convergence response, but the use of this instant information may be more sensitive to noise in steady-state.

Figs. 5 and 6 depict the torque estimation performance and the corresponding estimation errors. The performance indices are also shown in Table IV. It can be found that the adaptive law (54) with a time-varying learning gain has overall better

TABLE IV
TORQUE ESTIMATION PERFORMANCE INDICES

Index	Constant Gain		Time-varying Gain	
κ	$\kappa = 0$	$\kappa = 0.1$	$\kappa = 0$	$\kappa = 0.1$
ISE	1.5473e + 5	1.3263e + 5	1.7152e + 5	7.4863e + 4
MAE	19.2048	14.8248	19.6502	12.7438
SD	2.6222	2.4279	2.7607	1.8234

TABLE V
ENGINE SPECIFICATIONS

Property	Description
Engine type	Turbocharged diesel
Cylinder	4
Injection pressure	1400 bar
Compression ratio	16
Max Torque	320 N·m at 1800–2000 r/min
Max Power	95 kW at 3800 r/min
Capacity	1998 cc
Turbocharger	Garrett variable geometry

performance than the adaptive law (50) with a constant learning gain, i.e., the three indices are all smaller when including the time-varying gain K. This can be also reflected in Fig. 6(a) and (b) when comparing to Fig. 6(c) and (d). As we explained in Theorem 3, the time-varying gain K can compensate for the influence of matrix P and thus can improve the steady-state convergence response.

Furthermore, it is obvious that Fig. 6(b) and (d) contain more high frequency oscillations than Fig. 6(a) and (c) due to the use of W_2 with instant error information in (49), which is sensitive to noise as we analysed in Remark 6. However, the advantage of including W_2 can be seen in Fig. 6 that the peak errors at the transient points (e.g., 12 s and 24 s) in Fig. 6(b) and (d) are reduced compared to Fig. 6(a) and (c). This is also reflected from Table IV, which indicates that the ISE, MAE and SD are reduced when κ changes from 0 to 0.1. This proves that W_2 is beneficial to track fast time-varying dynamics. In these case, we also found that the estimated parameters $\theta_1(t)$ and $\theta_2(t)$ corresponding to N and $\dot{m}_{ai}$ are all bounded.

VII. PRACTICAL VALIDATION

This section will present the practical results based on an engine test rig with dynamometer to further validate the practical application of the proposed methods.

A. Description of Test Bench

The test engine is a turbocharged 2.0 L diesel engine with common rail direct injection, the specifications of which is presented in Table V. The engine incorporated a cooled high-pressure EGR system. The maximum torque is 320 N·m at 1800–2000 rpm and maximum power is 95 kW at 3800 rpm. It is mounted on a test bench and coupled to a McClure 215 kW transient dynamometer as shown in Fig. 7. The whole system is controlled using a CP CADET V14 control and data acquisition system.

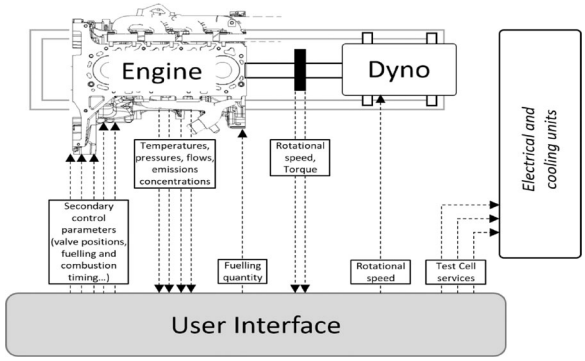

Fig. 7. Engine test bench used for experiments.

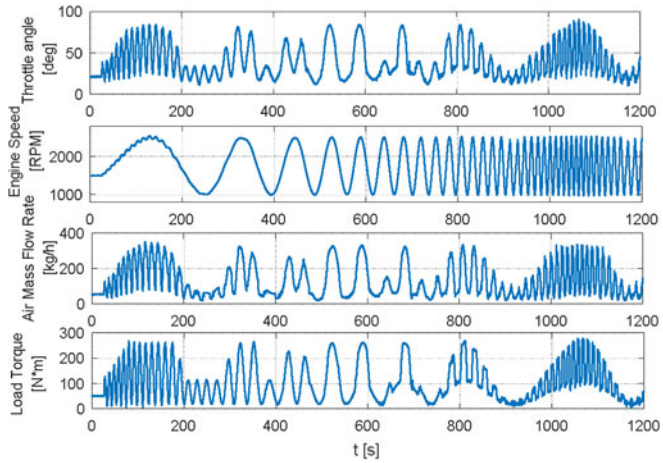

Fig. 8. Engine dynamic measurements in experiments.

B. Practical Results

Without loss of generality, we control the engine speed within 1000–2500 r/min and the applied load torque within 0–300 N·m during experiments. The engine dynamics are measured as presented in Fig. 8. Sine sweep excitation signals were used to vary the engine speed. The load with both slow and fast transient operating conditions is simulated [36] in the practical data collection experiments.

We first test the three UIO based torque estimators presented in Section III. The parameters used in these estimators are set as $k = 0.01$ and $\lambda_1 = 350$. Figs. 9 and 10 present the torque estimation results and errors. The performance indices are calculated using the data point from 5 s to 30 s, which are given in Table VI. It can be verified again that the proposed estimator (14) can obtain better performance compared to the sliding mode estimator (21) and the dirty differentiation estimator (24).

We finally test the adaptive laws for time-varying parameter estimation proposed in Section V, i.e., the adaptive law (50) with constant learning gain and the adaptive law (54) with time-varying learning gain. The parameters used in these adaptive laws are the same as those used in the above simulations. Fig. 11 presents the practical results of torque estimation errors. Table VII shows the corresponding performance indices.

It can be verified again that the adaptive law (54) with time-varying learning gain has better steady-state performance than adaptive law (50) with constant learning gain. Moreover, the use

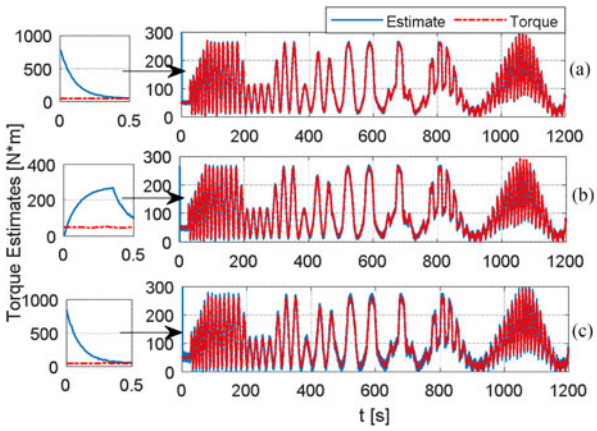

Fig. 9. Torque estimation with different methods. (a) UIO (14). (b) Sliding mode estimator (21). (c) Dirty differentiation estimator (24).

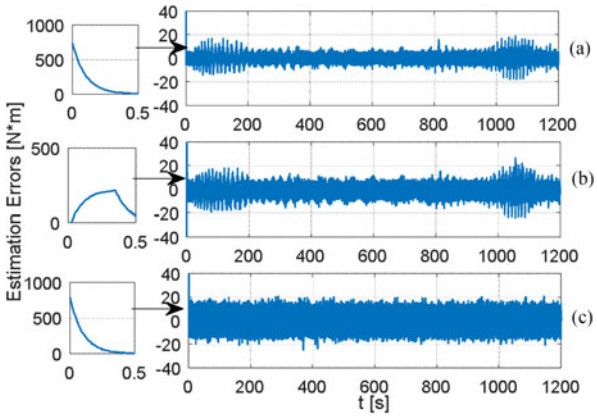

Fig. 10. Torque estimation errors with different methods. (a) UIO (14). (b) Sliding mode estimator (21). (c) Dirty differentiation estimator (24).

TABLE VI
TORQUE ESTIMATION PERFORMANCE INDICES

Index	UIO	Sliding mode	Dirty differentiation
ISE	1.5264e + 06	3.4639e + 06	4.2208e + 06
MAE	18.8252	26.5097	24.8369
SD	2.9120	4.2565	4.8424

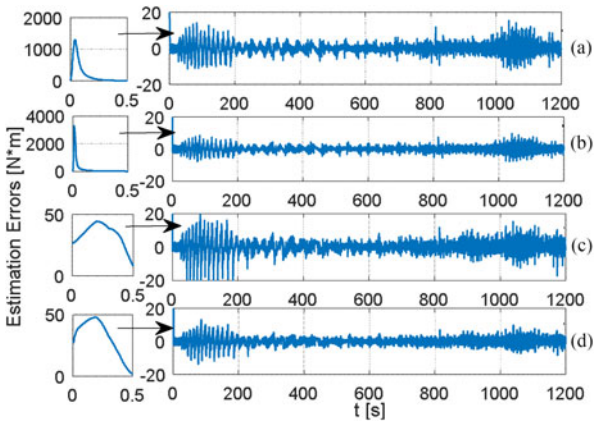

Fig. 11. Torque estimation with: (a) adaptive law (50) with $\kappa = 0$, (b) adaptive law (50) with $\kappa = 0.1$, (c) adaptive law (54) with $\kappa = 0$, and (d) adaptive law (54) with $\kappa = 0.1$.

TABLE VII
TORQUE ESTIMATION PERFORMANCE INDICES

Index	Constant Gain		Time-varying Gain	
κ	$\kappa = 0$	$\kappa = 0.1$	$\kappa = 0$	$\kappa = 0.1$
ISE	8.6268e + 5	3.0278e + 5	1.0647e + 6	3.5609e + 5
MAE	15.4241	9.4317	17.2514	9.6780
SD	2.1888	1.2967	2.4291	1.4044

of W_2 with instant error information may be sensitive to sensor noise, thus κ needs to be carefully set to obtain a trade-off between robustness and performance.

VIII. DISCUSSION

Practical and simulation results show that the UIO (14) can obtain better performance than the sliding mode estimator and the dirty differentiation estimator. The adaptive parameter estimator (54) with time-varying learning gain can even have better results than that (50) with constant gain. Furthermore, it is also interesting to compare the two different torque estimation methods, i.e., unknown input observer and parameter estimation. Clearly, the UIO (14) is simple and easy to implement. Only one parameter k needs to be selected. Hence, it requires less computational costs, which is more suited for practical applications. The adaptive parameter estimator (54) can provide smoother and improved estimation performance, because the engine dynamics (e.g., relationship between engine torque, speed and air mass) are considered in this scheme. Moreover, the latter one also provides some insights of the implicit relationship between the effective torque and the internal engine dynamics, i.e., the air mass flow rate and the engine speed. Nevertheless, the time-varying parameter estimation imposes a higher computational burden due to the online calculation of the auxiliary variables (e.g., P, Q, W_1, W_2 and K).

Moreover, the large peak errors encountered in the transient period (shown in above figures) are due to the fact that we set all initial estimation conditions as zero (e.g., $\hat{\Theta}(0) = 0$). Hence, there may be large transient errors before the proposed estimators achieve convergence. However, this transient process presented in this paper is very fast (e.g., less than 1 second). This phenomenon is quite normal for every estimation scheme presented in other papers (e.g., [11]). In fact, the transient estimation errors can be diminished if we have a priori information of the system parameters, which can help to set better initial errors (e.g., initialize $\hat{\Theta}(0)$ around its true values Θ) to reduce the transient errors.

IX. CONCLUSIONS

This paper addresses the online estimation of unknown effective engine torque with measured engine speed, load torque and air mass flow rate, and presents two different frameworks: unknown input observer (UIO) and time- varying parameter estimation. Thus, this paper presents a novel simple UIO and several adaptive laws. The first UIO only uses the engine crankshaft rotation dynamics, requests low-pass filter operations with only one tuning constant, and thus is simple for implementation. Both

the convergence and robustness of this UIO are compared with two other UIOs; it provides smoother performance and comparable robustness compared to sliding mode estimator. Considering the fact that the torque can be presented in a parameterized form, which has time-varying dynamics corresponding to the air mass flow rate and the engine speed, a novel adaptive parameter estimation algorithm is suggested to estimate such time-varying parameters. The essential feature of this adaptation is that it is driven by the parameter estimation error and uses time-varying learning gains. In this respect, the proposed adaptive laws can pave a potential way to solve the problem for time-varying parameter estimation in other applications. The proposed methods derived based on MVEM are generic, and thus they are applicable to different engines, e.g., port injection naturally aspirated gasoline engines, direct injection turbocharged gasoline engines, and turbocharged direct injection diesel engines. Moreover, these algorithms have been validated under realistic conditions. Both simulations based on an engine simulator built in commercial software (GT Power) and practical results based on a dynamometer test-rig are presented to support the theoretical studies. The small estimation errors also demonstrate the commercial potential of these algorithms.

REFERENCES

[1] M. N. Mahyuddin, J. Na, G. Herrmann, X. Ren, and P. Barber, "Adaptive observer-based parameter estimation with application to road gradient and vehicle mass estimation," *IEEE Trans. Ind. Electron.*, vol. 61, no. 6, pp. 2851–2863, Jun. 2014.

[2] J. Franco, M. A. Franchek, and K. Grigoriadis, "Real-time brake torque estimation for internal combustion engines," *Mech. Syst. Signal Process.*, vol. 22, pp. 338–361, 2008.

[3] D. Pavkovic and I. Kolmanovsky, "Adaptive Kalman filter-based load torque compensator for improved SI engine idle speed control," *IEEE Trans. Control Syst. Technol.*, vol. 17, no. 1, pp. 98–110, Jan. 2009.

[4] S. Helm, M. Kozek, and S. Jakubek, "Combustion torque estimation and misfire detection for calibration of combustion engines by parametric Kalman filtering," *IEEE Trans. Ind. Electron.*, vol. 59, no. 11, pp. 4326–4337, Nov. 2012.

[5] P. Niazi, H. A. Toliyat, and A. Goodarzi, "Robust maximum torque per ampere (MTPA) control of PM-assisted SynRM for traction applications," *IEEE Trans. Veh. Technol.*, vol. 56, no. 4, pp. 1538–1545, Jul. 2007.

[6] S. Bogosyan, M. Gokasan, and D. J. Goering, "A novel model validation and estimation approach for hybrid serial electric vehicles," *IEEE Trans. Veh. Technol.*, vol. 56, no. 4, pp. 1485–1497, Jul. 2007.

[7] N. Amano, "Method of calculating engine torque," US 20030204302 A1, 2004.

[8] G. Rizzoni, "Estimate of indicated torque from crankshaft speed fluctuations: A model for the dynamics of the IC engine," *IEEE Trans. Veh. Technol.*, vol. 38, no. 3, pp. 168–179, Aug. 1989.

[9] G. Rizzoni, S. Drakunov, and Y.-Y. Wang, "On-line estimation of indicated torque in IC engines via sliding mode observers," in *Proc. 1995 Amer. Control Conf.*, 1995, pp. 2123–2127.

[10] Y. Wang, V. Krishnaswami, and G. Rizzoni, "Event-based estimation of indicated torque for IC engines using sliding-mode observers," *Control Eng. Pract.*, vol. 5, pp. 1123–1129, 1997.

[11] Q. R. Butt and A. I. Bhatti, "Estimation of gasoline-engine parameters using higher order sliding mode," *IEEE Trans. Ind. Electron.*, vol. 55, no. 11, pp. 3891–3898, Nov. 2008.

[12] Q. Ahmed and A. I. Bhatti, "Estimating SI engine efficiencies and parameters in second-order sliding modes," *IEEE Trans. Ind. Electron.*, vol. 58, no. 10, pp. 4837–4846, Oct. 2011.

[13] J. Chauvin, G. Corde, P. Moulin, M. Castagné, N. Petit, and P. Rouchon, "Real-time combustion torque estimation on a diesel engine test bench using an adaptive Fourier basis decomposition," in *Proc. 43rd IEEE Conf. Decision Control*, 2004, pp. 1695–1702.

[14] J. Chauvin, G. Corde, P. Moulin, M. Castagné, N. Petit, and P. Rouchon, "Real-time combustion torque estimation on a diesel engine test bench using time-varying Kalman filtering," in *Proc. 43rd IEEE Conf. Decision Control*, 2004, pp. 1688–1694.

[15] P. Falcone, G. Fiengo, and L. Glielmo, "Non-linear net engine torque estimator for internal combustion engine," in *Proc. IFAC Symp. Adv. Autom. Control*, 2004, pp. 125–130.

[16] P. Falcone, G. Fiengo, and L. Glielmo, "Nicely nonlinear engine torque estimator," in *Proc. IFAC World Congr.*, vol. 38, 2005, pp. 218–223.

[17] M. Hong, T. Shen, M. Ouyang, and J. Kako, "Torque observers design for spark ignition engines with different intake air measurement sensors," *IEEE Trans. Control Syst. Technol.*, vol. 19, no. 1, pp. 229–237, Jan. 2011.

[18] A. Stotsky and I. Kolmanovsky, "Application of input estimation techniques to charge estimation and control in automotive engines," *Control Eng. Pract.*, vol. 10, pp. 1371–1383, 2002.

[19] A. Stotsky, I. Kolmanovsky, and S. Eriksson, "Composite adaptive and input observer-based approaches to the cylinder flow estimation in spark ignition automotive engines," *Int. J. Adapt. Control Signal Process.*, vol. 18, pp. 125–144, 2004.

[20] J.-J. E. Slotine and W. Li, *Applied Nonlinear Control*, vol. 199. Englewood Cliffs, NJ, USA: Prentice-Hall, 1991.

[21] P. A. Ioannou and J. Sun, *Robust Adaptive Control*. North Chelmsford, MA, USA: Courier Corporation, 2012.

[22] M. de Mathelin and R. Lozano, "Robust adaptive identification of slowly time-varying parameters with bounded disturbances," in *Proc. 1997 Eur. Control Conf.*, 1997, pp. 2300–2305.

[23] I. Kolmanovsky, I. Sivergina, and J. Sun, "Simultaneous input and parameter estimation with input observers and set-membership parameter bounding: Theory and an automotive application," *Int. J. Adapt. Control Signal Process.*, vol. 20, pp. 225–246, 2006.

[24] J. Na, G. Herrmann, R. Burke, and C. Brace, "Adaptive input and parameter estimation with application to engine torque estimation," in *Proc. IEEE Conf. Decision Control*, Osaka, Japan, 2015, pp. 3687–3692.

[25] E. Hendricks and J. Luther, "Model and observer based control of internal combustion engines," in *Proc. Int. Workshop Model. Emissions Control Autom. Engines*, 2001, pp. 9–20.

[26] E. Hendricks and S. C. Sorenson, "Mean value modelling of spark ignition engines," SAE Tech. Paper, 1990.

[27] A. Astolfi and R. Ortega, "Immersion and invariance: A new tool for stabilization and adaptive control of nonlinear systems," *IEEE Trans. Autom. Control*, vol. 48, no. 4, pp. 590–606, Apr. 2003.

[28] J. Na, G. Herrmann, X. Ren, M. N. Mahyuddin, and P. Barber, "Robust adaptive finite-time parameter estimation and control of nonlinear systems," in *Proc. IEEE Int. Symp. Intell. Control*, 2011, pp. 1014–1019.

[29] J. Na, M. N. Mahyuddin, G. Herrmann, and X. Ren, "Robust adaptive finite-time parameter estimation for linearly parameterized nonlinear systems," in *Proc. 2013 32nd Chin. Control Conf.*, 2013, pp. 1735–1741.

[30] J. Na, M. N. Mahyuddin, G. Herrmann, X. Ren, and P. Barber, "Robust adaptive finite-time parameter estimation and control for robotic systems," *Int. J. Robust Nonlinear Control*, vol. 25, pp. 3045–3071, 2015.

[31] G.-P. U. s. Manual, "GT-Suite version 7.3," 2012.

[32] M. Fam and E. Hendricks, "A load torque estimator," SAE Tech. Paper 0148-7191, 2004.

[33] Z. Zhao, X. Li, L. He, C. Wu, and J. K. Hedrick, "Estimation of torques transmitted by twin-clutch of dry dual clutch transmission during vehicle's launching process," *IEEE Trans. Veh. Technol.*, vol. 66, no. 6, pp. 4727–4741, Jun. 2017.

[34] J. J. Oh and S. B. Choi, "Real-time estimation of transmitted torque on each clutch for ground vehicles with dual clutch transmission," *IEEE/ASME Trans. Mechatronics*, vol. 20, no. 1, pp. 24–36, Feb. 2015.

[35] C. Edwards and S. Spurgeon, *Sliding Mode Control: Theory and Applications*. Boca Raton, FL, USA: CRC Press, 1998.

[36] R. D. Burke, W. Baumann, S. Akehurst, and C. J. Brace, "Dynamic modelling of diesel engine emissions using the parametric Volterra series," *Proc. Inst. Mech. Eng. Part D: J. Autom. Eng.*, vol. 227, pp. 1–16, 2013.

[37] P. Zhu, Y. Zhang, and G. L. Chen, "Metamodel-based lightweight design of an automotive front-body structure using robust optimization," *Proc. Inst. Mech. Eng. Part D: J. Autom. Eng.*, vol. 223, no. 9, pp. 1133–1147, 2009.

[38] M. S. Kompella and R. J. Bernhard, "Measurement of the statistical variation of structural-acoustic characteristics of automotive vehicles," SAE Tech. Paper 931272, 1993.

Authors' photographs and biographies not available at the time of publication.